

Article

Strength and Microstructure of Coffee Silverskin Blended Mortar

Moruf Olalekan Yusuf ^{1,*}, Zeyad M. A. Mohammed ¹, Adeshina A. Adewumi ¹, Mutasem Taisir Shaban ¹, Meshrif Omar Meshrif AlBaqawi ¹ and Hatim Dafalla Mohamed ²

¹ Department of Civil Engineering, College of Engineering, University of Hafr Al Batin, Hafr Al Batin 39524, Saudi Arabia

² Core research Facilities, Research Institute, King Fahd University of Petroleum and Minerals, Dhahran 31261, Saudi Arabia

* Correspondence: moruf@uhb.edu.sa; Tel.: +966-552545213

Abstract: This study pertains to incorporation of coffee silverskin (CSS) in partial replacement for ordinary Portland cement (OPC) in mortar, by investigating its fresh properties (setting and workability), compressive strength (3, 7, 14 and 28-day), absorption and microstructural characteristics. The objectives were to reduce environmental solid wastes and achieve cost efficiency in the use of construction materials. The CSS was expressed as a ratio of total binder (CSS/(OPC + CSS)) and varied from 0 to 5%. The findings revealed that CSS could reduce workability, setting time and early strength. It could also enhance the absorption of the CSS-blended mortar (CBM). The cause of reduction in workability was due to its contribution to the viscosity of the mixture due to the emulsification of the fat component (acetate) and aromatic compounds, as observed in the Fourier Transform Infrared (FTIR) spectroscopy and X-ray diffraction techniques. The presence of these compounds also caused microstructural disintegration that resulted in the lower strength. In addition, the presence of other organic compound in CSS but absent in OPC enhanced microstructural disintegration and porosity in CBM. The 28-day strength of 25 MPa could be achieved in CSS-blended mortar if the CSS/(CSS + OPC) ratios were kept below 3%. The maximum compressive strength of 38.5 MPa was obtained with the optimum CSS content of 1 wt%. The relative density (water) of CSS was 0.345; therefore, it could also be used to produce lightweight concrete. This study promotes the valorization of raw CSS waste as construction material which could be used for subgrade in the construction of road pavement.

Keywords: coffee silverskin; compressive strength; setting; workability; microstructural and bond characteristics



Citation: Yusuf, M.O.; Mohammed, Z.M.A.; Adewumi, A.A.; Shaban, M.T.; AlBaqawi, M.O.M.; Mohamed, H.D. Strength and Microstructure of Coffee Silverskin Blended Mortar. *Recycling* **2022**, *7*, 59. <https://doi.org/10.3390/recycling7040059>

Academic Editor: Eugenio Cavallo

Received: 6 July 2022

Accepted: 12 August 2022

Published: 15 August 2022

Publisher's Note: MDPI stays neutral with regard to jurisdictional claims in published maps and institutional affiliations.



Copyright: © 2022 by the authors. Licensee MDPI, Basel, Switzerland. This article is an open access article distributed under the terms and conditions of the Creative Commons Attribution (CC BY) license (<https://creativecommons.org/licenses/by/4.0/>).

1. Introduction

Coffee belongs to the family of *Rubiaceae* and is categorized into three different species, namely: *Coffea arabica*, *Coffea robusta* and *Coffea liberica*. Coffee is mostly grown in East Africa, South America and India, with Brazil having the largest global production [1]. Coffee is an item of trade in the consumer market of about 30 million sacks per year [2]. At the same time, the industry is a potential source of biomass wastes with the global consumption of 9.68 billion kilograms in 2017–2018. The annual world production of coffee generated over 10 million tons of residues from discarded cherries (bean, mucilage, pulp and shell) and shrubs [3]. The consumption of coffee-dependent beverages during 2021 spiked by 1.3%, which amounted to 166 million bags (9978 million kg) [4].

A coffee bean in its green state has an outer layer of 68% pulp (exocarp and mesocarp) and 6–10% parchment (endocarp) [5]. Its green wastes include parchment pulps and husk (Figure 1A), which account for 29% of the whole cherry [6]. The parchment itself comprises 54% cellulose, 27% pentosans and 19% lignin [7]. It has been estimated that 1 ton of pulp (Figure 1B) is generated for every 2 tons of commercially processed coffee [8]. Post-treated (roasted) coffee wastes include coffee silverskin (CSS) and spent coffee ground (SCG).

Roasted coffee bean is much more available in the coffee-consuming countries (Arabian gulf region) and generates abundant CSS (Figure 1C) and SCG (Figure 1D).



Figure 1. Pictorial view of (A) Coffee husk (CH), (B) coffee pulp (CP), (C) coffee silverskin (CSS), and (D) spent ground coffee (SCG) Source: [6].

SCG's polygonal shape is obtained from brewed coffee and constitutes 91% of ground coffee. CSS is a flat shape (Figure 2) that is made from the low mass tegument of coffee, and it is about 4.2% of the total coffee bean. It is rich in phenolic compounds, antioxidants, soluble dietary fiber and poly-unsaturated fatty acid, thereby making it a good raw material for cosmetics and skin gel [9]. CSS has larger lignin composition and more cellulose than SCG, which has more hemicellulose in turn [10]. The nutritional composition of CSS has a wide range constituents such as fiber (56.4–74.2%), insoluble dietary fiber (48.5–66.9%), soluble dietary fiber (3.3–8.8%), protein (11.8–19.0%), fat (2.1–5.8%), lignin (17.8–31%), ash (4.5–8.3%), cellulose (10.3–23.8%), hemicellulose (7.5–16.7%) and caffeine (0.91–1.40%) [11]. Both SCG and CSS have nutritional compositions that comprise lignin, protein, low fat and polysaccharide sugar in the forms of cellulose and hemicellulose. SCG is also used in various application such as biofuel, antioxidants, bioethanol, biodiesels or biofuel [12] and as a sugar source, a spirit and as substrate for mushroom production [3,8,10]. They also have similar melting points, high water-holding capacities and low porosity [13].



Figure 2. Pictorial view and SEM of coffee silverskin (CSS1-bottom) and spent ground coffee (SCG1-top) Source: [10].

Aluminosilicate minerals are very essential in the production of mortar and concrete [14]. It has been shown that coffee ground husk (CGH) ash contains no aluminosilicate oxides, TiO_2 or Fe_2O_3 . The absence of these oxides limits the utilization of CGH to promote

strength in concrete. The authors of [15] saw the possibility of extracting caustic potash through potassium carbonate from CGH. In light of this, 5 wt% of CGH ash was added to concrete in the mix ratio 0.5:0.5:1:0.5 for gravel, sand, cement and water, respectively, to achieve a 28-day strength of 20 MPa [2]. Furthermore, [16] investigated the effect of coffee peels on the porosity and density of construction bricks, and the results showed a decrease in strength coupled with better insulation property. Moreover, [17] also used CGH ash in concrete production at the substitution level of 5–25 vol% to achieve a maximum 28-day strength of 23 kPa when CGH/(CGH + OPC) ratio was 5%. They observed a reduction in the density and an extension of initial and final setting times to 168 and 305 min, respectively. This implies that CGH can be used as retarder in the cementing oil rig and in concrete production [18]. Moreover, [19] used SCG in two binder typologies—geopolymer and ordinary hydraulic lime—for sustainable building. They reported high absorption and better thermal insulation despite the significant reduction in strength when OPC was replaced by 5 wt%. The authors of [20] combined SCG with flyash and slag in the synthesis of alkaline activated binder to achieve a dry unit weight of 8.9 kN/m³ and a maximum strength of 1.2 MPa.

Despite these studies on CGH and SCG, there is no study yet in the literature on the performance of CSS in mortar production. It is also salient to note that disposal of CSS by burning could generate hazardous contaminants such as NO_x [21]. An attempt to also pelletize it as biofuel produced particulate that could aggravate air pollution, and that could endanger public health. Therefore, there is a need to find an alternative way of utilizing it, for instance, as a construction material effectively. Furthermore, there is also a need to understand the effective use of CSS as partially substituted material for OPC (0–5 wt%) in mortar production. It is also essential to examine the characteristics of such mortar and its fresh, hardening (compressive strength), absorption, mineral phases and microstructural/bond characteristics using scanning electron microscope/energy dispersive spectroscopy (SEM/EDS), Fourier transform infrared spectroscopy (FTIR) and X-ray diffraction (XRD) techniques.

2. Material and Methods

2.1. Materials

2.1.1. Coffee Silverskin (CSS)

Coffee silverskin (CSS) from *Coffea arabica* was collected from coffee processing shops within the city of Hafr Al Batin in Saudi Arabia. It was then milled and sieved through a 500-micron aperture sieve. CSS's relative density (water) is 0.345 while the surface area by BET is 3215.3 m²/kg with adsorption pore volume of 12.54 cm³/kg. Figure 3 shows the Fourier Transform Infrared (FTIR) spectroscopy of CSS.

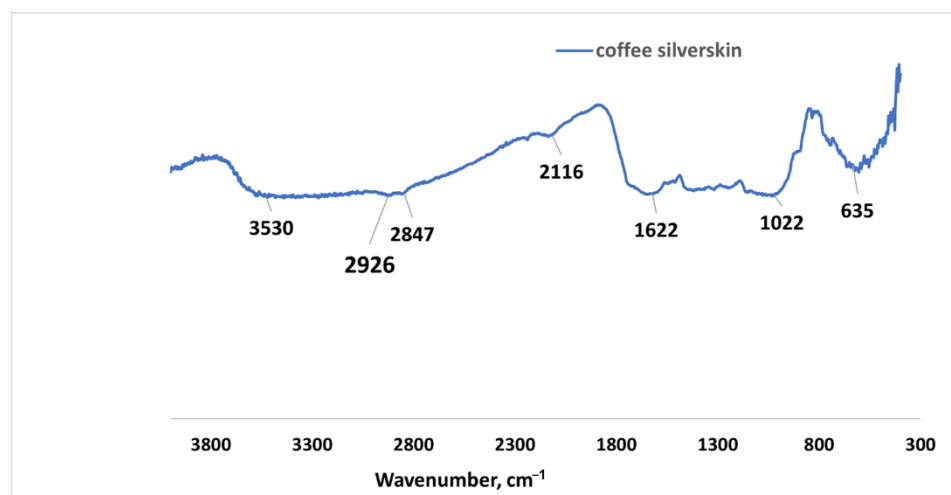


Figure 3. FTIR spectra for raw coffee silverskin.

2.1.2. Ordinary Portland Cement

Type 1 cement was used in accordance with ASTM C 150 [22] with apparent specific gravity (water) of 3.15. Oxides composition of OPC together with other materials are as shown in Table 1. X-ray diffraction (XRD) of dry powder cement and CSS are shown in Figure 4.

Table 1. Oxide composition of cement and coffee silver skin.

Oxides (%)	Cement	CSS
SiO ₂	20.2	2.72
Al ₂ O ₃	4.6	5.09
Fe ₂ O ₃	2.9	5.48
CaO	62.5	29.61
MgO	3.2	0.00
Na ₂ O	0.6	0.00
K ₂ O	0.6	56.11
SO ₃	2.6	0.38
P ₂ O ₅	0.2	0.02
TiO ₂	0.1	0.32
MnO	0.0	0.28
Cr ₂ O	2.4	0.00
SiO ₂ + Al ₂ O ₃ + Fe ₂ O ₃	27.7	13.3
Specific gravity (water)	3.1	0.35
Specific surface area (m ² /kg)	329.5	3215.30
LOI (wt%)	2.8	1.30

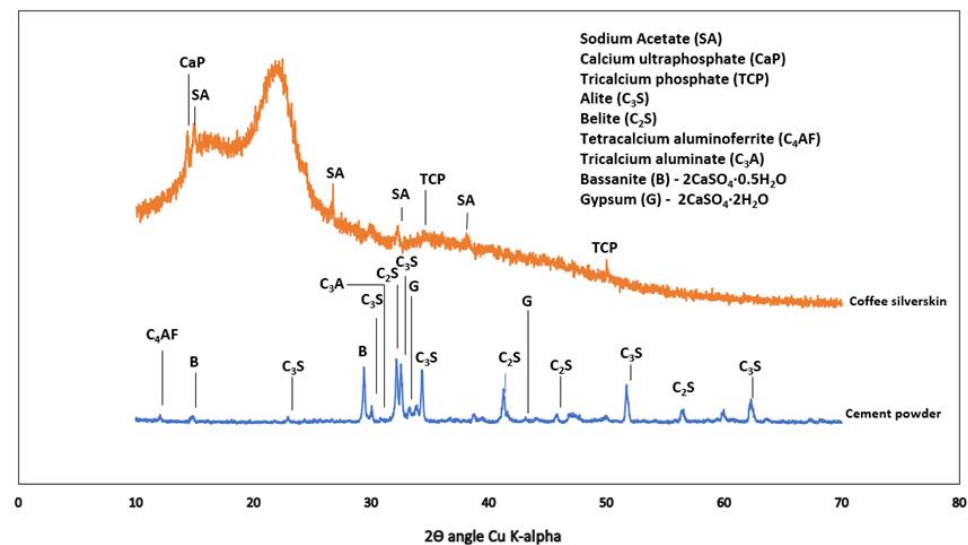


Figure 4. X-ray diffractogram of coffee silverskin and cement powder.

2.1.3. Superplasticizer

Glenum 51[®] superplasticizer based on modified polycarboxylic ether was supplied by BASF, Germany. It complies with ASTM C 494 Types A and F, while 0.5 wt% of total binder was used to achieve better workability of the mortar.

2.1.4. Fine Aggregates

Natural sand was used in the production of the coffee-silverskin-blended mortar. It passes the sieve no 2.36 mm (No. 8) in accordance with ASTM C 157 [23]. The specific gravity (water) is 2.71, while its fineness modulus was 2.8.

2.2. Experimental Tests

2.2.1. Workability

The workability was determined using paste specimen prepared at water/binder ratio of 0.26 by using the flow table with the measurement of the spread after 25 blow counts in accordance with ASTM C 1437 [24].

2.2.2. Setting Time

The initial and final setting times of the cement–CSS blended paste was determined in accordance with ASTM C191 [25] by using a water/binder ratio of 0.26.

2.2.3. Water Absorption

Water absorption of the sample size 50 mm × 50 mm × 50 mm was determined by submerging the sample in water for 7 days and then measured its saturated surface dry weight (M_{ssd}). It was then placed inside oven at temperature of 105 °C for 24 h (M_{oven}) in accordance with ASTM C 1403 [26]. The percentage absorption is as shown in Equation (1):

$$\text{Water absorption} = \frac{M_{ssd} - M_{oven}}{M_{oven}} \times 100 \tag{1}$$

2.2.4. Compressive Strength

Compressive strength of the mortar samples was determined using cubic samples of 50 mm sides in accordance with ASTM C109 [27]. The testing was performed by universal testing machine using the loading rate of 0.9 kN/s. The average of triplicate samples was recorded at 3, 7, 14 and 28 days as the compressive strengths.

2.3. Characterization and Morphology of the Specimens

To determine the bond behavior, morphology and nature of mineral phases in the products, Fourier transform spectroscopy (FTIR) spectrometer made by PerkinElmer 880 Inc., (Norwalk, CT, USA); scanning electron microscopy/energy dispersive X-ray spectroscopy (SEM + EDS) SEM + EDS model 5800 LV operated at accelerating voltage of 20 kV made by JEOL, Rueil-Malmaison, France; and X-ray diffractometer (XRD) machine manufactured by Bruker instrument (Billerica, MA, USA), model d2-Phaser with Cu Ka radiation (40 kV, 40 mA) were used, respectively. The samples were continuously scanned within angle 2-theta range of 10–80° and at a scan speed of 2.5°/min. The phases were identified using Profex® software [28]. Surface area and pore sizes distribution was determined by BET Micromeritic instrument (Norcross, GA, USA), with the sample size 0.2 g of N₂ adsorption at 77k temperature.

2.4. Sample Preparation

2.4.1. Sample Designation

Each sample denoted by Cm_{100-x}C_x indicating the quantity of cement (Cm) and coffee silverskin (CSS) with $x = \text{CSS}/(\text{CSS} + \text{Cm})$ that varies as 0, 0.5, 1, 1.5, 2, 3, 4 and 5 w% with the equivalent volume ratios of 0, 5, 10, 14, 19, 28, 38 and 48 vol%, respectively (Table 2).

Table 2. Mix design for coffee (CSS) blended mortar.

Sample	Total Binder kg/m ³	Coffee Weight (wt%)	Cement Content (%)	Sand/Binder Ratio (wt)	Water/Binder Ratio (wt)	SP (% of Binder)
Cm _{100-x} C _x	350	x	100-x	2.75	0.40	0.5

2.4.2. Mix Design

Mortar samples were made based on the mix design shown in Table 3. The water–binder ratio was maintained at 0.40 with the addition of 2% absorption from fine aggregates

to maintain saturated surface dry (SSD) condition. The total mass of the binders (cement with coffee silverskin) in 1 m³ of the mortar content was 350 kg.

Table 3. Mix design for coffee silverskin blended mortar.

Sample	Coffee Content (by wt%)	Coffee Content (by vol%)	Cement Kg/m ³	Coffee Kg/m ³	Sand Kg/m ³	Water Kg/m ³	SP Kg/m ³
Cm ₁₀₀ C ₀	0.0%	0.0%	350.00	0.00	962.50	138.25	17.5
Cm _{99.5} C _{0.5}	0.5%	4.6%	348.25	1.75	962.50	138.25	17.5
Cm ₉₉ C _{1.0}	1.0%	9.2%	346.50	3.50	962.50	138.25	17.5
Cm _{98.5} C _{1.5}	1.5%	13.9%	344.75	5.25	962.50	138.25	17.5
Cm ₉₈ C _{2.0}	2.0%	18.6%	343.00	7.00	962.50	138.25	17.5
Cm ₉₇ C _{3.0}	3.0%	28.2%	339.50	10.50	962.50	138.25	17.5
Cm ₉₆ C _{4.0}	4.0%	37.2%	336.00	14.00	962.50	138.25	17.5
Cm ₉₅ C _{5.0}	5.0%	46.5%	332.51	17.49	962.50	138.25	17.5

2.4.3. Mortar Mixing Procedure

Mixing was performed with the aid of rotary mixer by first adding cement and coffee silverskin (CSS) powder and in accordance with ASTM C 192 [29]. Half quantity of water that has been premixed with superplasticizer was then added and then mixed for 3 min. Fine aggregates (sand) were then added and mixed for another 3 min before adding the remaining water. The mixture was then mixed for 4 min before being cast in the oil smeared molds in two layers. The sample was vibrated for 15 s, and leveled with the edge of the mold by using a trowel before being covered with polythene sheet to prevent moisture loss. The specimens were placed in the laboratory at 20 ± 5 °C for 24 h before being demolded and placed inside the curing tank for a specific age (3, 7, 14 and 28 days) for the compressive strength test.

3. Discussion of Results

3.1. Characteristic of Coffee Silverskin

Figure 3 shows the FTIR spectroscopy analysis of raw CSS. The prominent peaks are noted at 3530 cm⁻¹, which could be ascribed to the hydroxyl group stretching vibration that could be found in ethanol or other phenolic compound present in CSS. The band at 2847 cm⁻¹ is ascribed to C-H stretching vibration of methyl (CH₃) in the organic compounds such as protein, lignin, and cellulose. This band has been reported by [30] in *Coffea arabica* and *robusta* to be due to the presence of methyl group in caffeine molecules [10]. The presence of amide within the protein content of CSS is responsible for the C-N stretching vibration band at 2116 cm⁻¹ [11], while the band at 1622 cm⁻¹ points to the C=O stretching vibration of carbonyl attached to aromatic compounds such as lignin [31]. This band is also connected to chlorogenic acid and caffeine in CSS [32]. The vibration at 1022 cm⁻¹ of alkoxy group (C-O) in C-O-H glycosidic bonds are connected to galactomannans polysaccharide sugar [33]. The C-H bending vibration band observed at 635 cm⁻¹ corresponds to aromatic compounds (lignin) [10].

The X-ray diffraction in Figure 4 shows the presence of sodium acetate (CH₃-C=O(ONa)), COD: #1549467), calcium ultra-phosphate (CaP-Ca₂O₁₇P₆, COD ID: #8104400) and tricalcium phosphate (TCP-Ca₃(PO₄)₂-COD ID: #1517238). It has been reported in [34] that ethanol and ethyl acetate could also be obtained from CSS as extracts, with caffeine as the major compound. The raw ordinary Portland cement comprises tetracalcium aluminoferrite (COD: #1008124), tricalcium silicate or alite (COD ID: #1540705), dicalcium silicate or belite (COD: #9012789), gypsum (COD: #1010981) and bassanite (COD: #9012208).

3.2. Workability of Coffee-Silverskin-Blended Mortar

Coffee silverskin has been reported to be less susceptible to hydrolysis due to its high composition of cellulose, which is more crystalline than hemicellulose. The presence of other organic compounds such as protein, lignin and fat could be responsible for the low consistency of the mixture. Furthermore, CSS has been reported [10] to have a higher water

and oil holding capacity of about 5.11%, thereby making water unavailable for interparticle lubrication and flow [35,36]. Another factor that caused the low workability of the mixture is the flat shape of CSS, as revealed in its morphology presented in Figure 2, such that particles could not move over one another but rather stick with one another [35,36].

In Figure 5, the consistency of the mortar sample decreases exponentially with the content of coffee silverskin (CSS). This is possible since the reaction of alkaline in pore solution could cause the emulsification of the fat present in CSS, thereby increasing the viscosity of the mixture on one hand and decreasing the interparticle mobility on the other. It could be observed that the higher the CSS/(CSS + OPC) ratio, in the mortar, the lower the consistency of the mixture. For instance, when the CSS/(CSS + OPC) ratios were 0.5, 2 and 5, the workability of the mortar decreased by 8.8%, 23% and 26.5%, respectively. It could also be seen that the difference between the result obtained from the ratios of 1 and 1.5 was just a decrease of 1.18%. Furthermore, there is no significance change in the workability of the sample when the CSS content is more than 1.5 wt%. This could be due to the stickiness of the CSS to the OPC particle, thereby preventing the flowability.

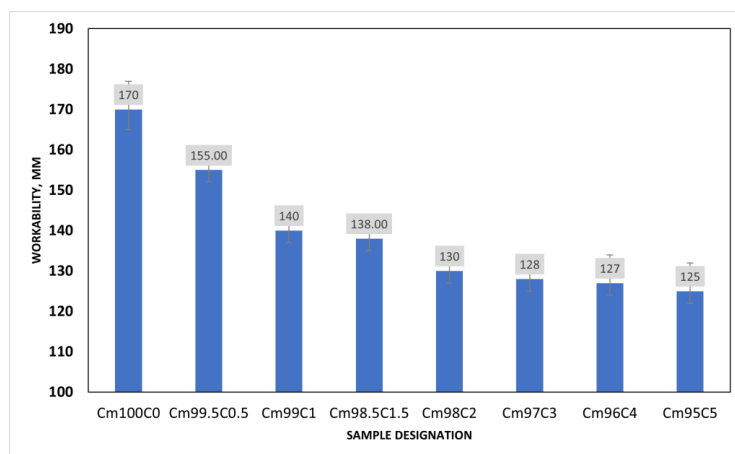


Figure 5. Workability of coffee silverskin blended mortar.

3.3. Effect of Coffee Silverskin on the Setting of the Blended Mortar

The setting of ordinary Portland cement is controlled by the reaction of C_3A with gypsum. The lack of enough gypsum could cause quick setting while the presence of fat, ethanol, hemicellulose, and sodium acetate in CSS could also prevent the mobility and hydration of C_3A , C_3S and C_2S in the early stage of hydration. The presence of these organic compounds could also disrupt the nucleation site, thereby preventing agglomeration of CSH. Unlike spent coffee ground (SCG), roasted CSS contains less sugar (mannose, galactose, arabinose and xylose), and its crystalline nature with straight chain could reduce retardation significantly [10]. From Figure 6, the setting time is decreasing with CSS exponentially. The initial setting time (85 min) of OPC mortar decreases with CSS content such that the inclusion of 0.5, 1.0, 1.5 and 2 wt% lowers the setting time by 17.6, 29.4, 57.6 and 62.3%, respectively. The difference in the initial setting of the CSS-blended mortar (CBM) for 1–2 wt% CSS partial cement replacement is not significant, while the final setting time was noticeably decreased by 23.4%. As the CSS/binder ratio increased to 0.5, 1, 1.5, 2, 3, 4 and 5wt%, the final setting time was observed to decrease by 33.3%, 51.1%, 57%, 65.1%, 76.7%, 83% and 88.9%, respectively. The decrease in setting time could also be adduced to the presence of calcium phosphate, and the water holding capacity of CSS could limit the mobility of gypsum and the amount of water available for hydration. The consequence of this led to quick C_3A hydration that caused early setting

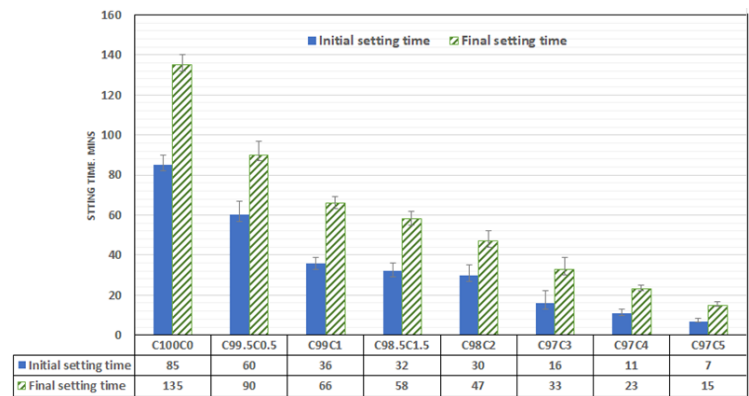


Figure 6. Setting time of coffee-silver-skin-blended mortar.

The asymmetric stretching of the S-O bond peak from sulfate-based compound (Aft) at 1115 cm^{-1} in OPC (cement), as shown in Figure 7, was observed to be distorted in CBM as the frequency of the S-O vibration reduced, as indicated by the wavenumber 1091 cm^{-1} [37]. The presence of anhydrite (CaSO_4 -COD #5000040) in Figure 8 implies that the presence of organic compounds prevented the complete hydration of C_3A , which led to the faster setting. This also supports less formation of Aft by observing the morphology of CBM (Figure 9A).

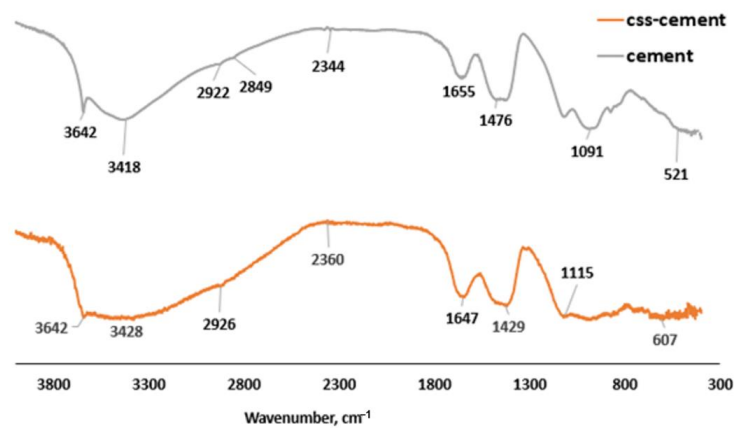


Figure 7. FTIR spectra for CSS-blended mortar and OPC mortar.

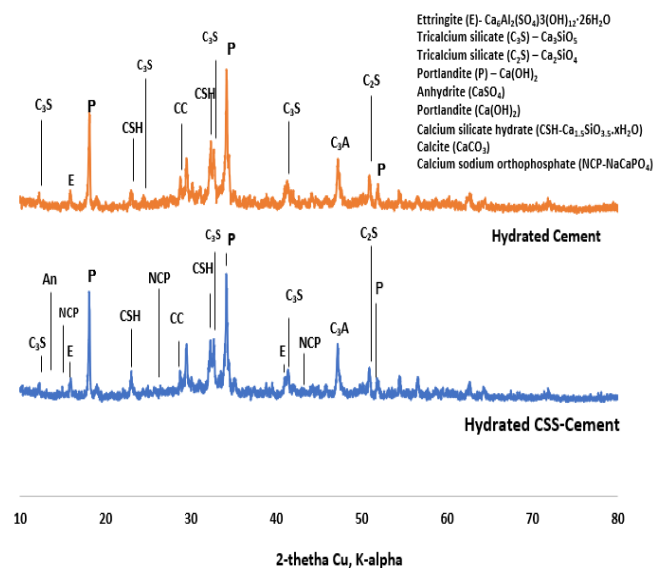
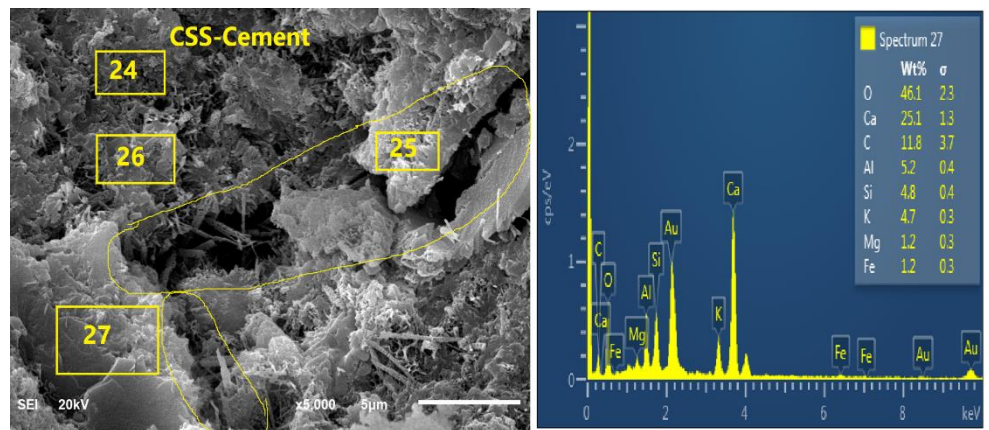
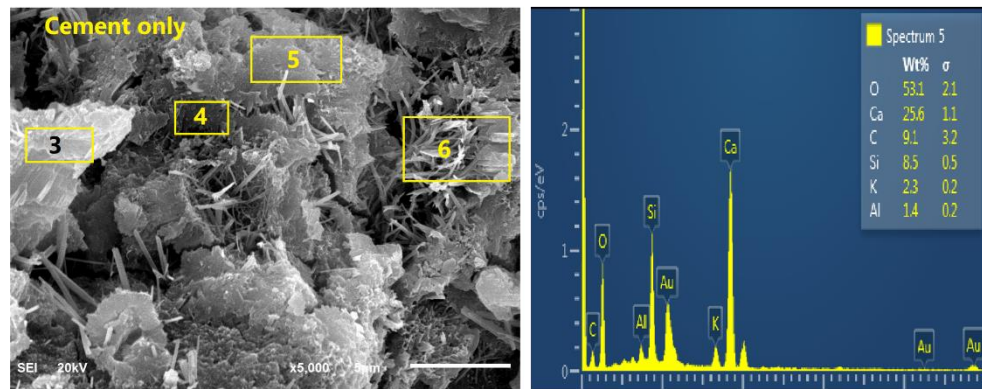


Figure 8. X-ray diffractogram of coffee-silverskin-blended (top) and cement paste (bottom).



A: CSS-Cement Mortar



B: Cement Mortar (CSS free)

Figure 9. Morphology of CSS-blended mortars (A-top) and OPC mortar (B-bottom).

3.4. Effect of Coffee Silverskin on the Compressive Strength of the Blended Mortar

The compressive strength decreases with the content of CSS (Figure 10). This implies that the early setting time observed in the CSS-blended mortar does not translate into early strength development. The reduction in early strength could be due to the presence of weak NaCaPO_4 (NCP-COD ID: #9011347), as noticed in the XRD (Figure 8), and other organic compounds such as fat, cellulose, lignin and protein present in CSS.

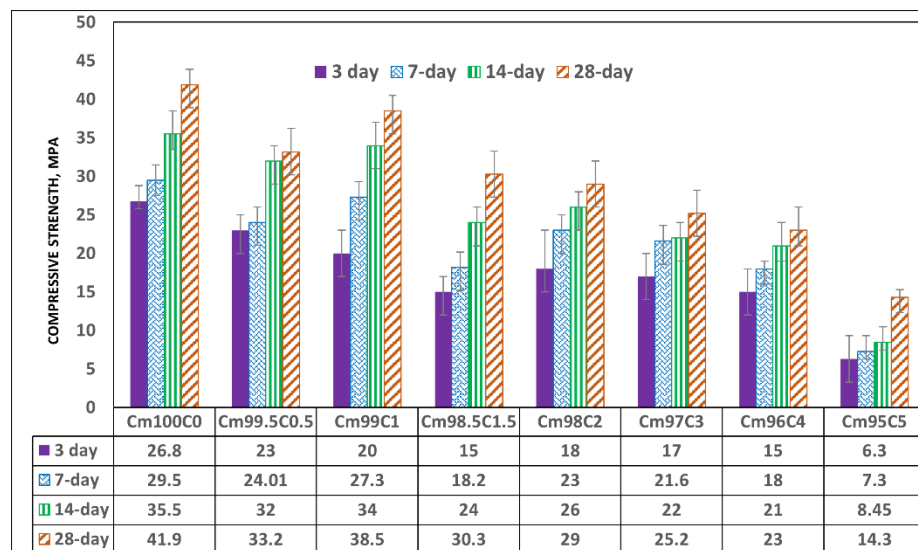


Figure 10. Compressive strength of coffee-silverskin-blended mortar.

The formation of these compounds causes weakness in the microstructure of the CSS-blended mortar (CBM), as shown in Figure 9, in comparison with OPC mortar (CSS-free). The interaction of CSS with the alkaline pore solution of OPC breaks the C-H bond of the CSS. This assertion is proven by the disappearance of the C-H stretching vibration band at 2847 cm^{-1} in raw CSS (Figure 7) that disappeared in CBM (Figure 3). The XRD of CSS-Cement blended mortar is similar to OPC mortar, except for the formation of NCP (COD ID: #9011347) and anhydrite within the products of CSH (COD# 9001689), portlandite (COD:#1001768) and calcite (COD: #1010928).

Early strength is seen to be decreasing linearly down to 44% when the CSS/binder ratio was 1.5 and reduced by 32.3%, 36.5%, 44.8% and 77.3% when the ratio became 2, 3, 4 and 5%, respectively. The 28-day compressive strength of 41.9 MPa was obtained in OPC mortar (zero CSS), which decreased by 21% and 8.1% when the CSS/binder ratios were 0.5 and 1%, respectively. The achievable strength further reduced to 45.1% and 66.9% when the CSS content was 4 wt% and 5 wt%, respectively. There was also no significant gain in strength between 3 and 14 days when CSS was 5 wt% due to the impeding hydration reaction that led to weak microstructural stability, as shown in Figure 9A. It was also observed that organic compounds present in the CSS did not stop the hydration reaction and strength development with time but only slowed its rate down. This is evident as all specimens—regardless of the content of CSS—have higher strength values at 28 days compared to the early strength recorded in 3 days (Figure 10).

By comparing spectrum 5 with 27, it is very evident that the higher the Ca/K and Ca/C ratios, the compressive strength in CSS-blended cement due to the higher content of potassium (K) and organic compounds (carbon-C). For instance, from Table 4, the Ca/K ratios in CBM and CSS-free mortar were 11.13 and 5.34, while the Ca/C ratios were 2.81 and 2.24, respectively. In contrast, the higher the Ca/Si ratios in the system, the lower the compressive strength. The Ca/Si ratios in CBM and OPC mortars were 3.08 and 5.23, respectively. There is also more needle-like Aft (ettringite, $\text{Ca}_6\text{Al}_2(\text{SO}_4)_3(\text{OH})_{12}\cdot 26\text{H}_2\text{O}$ -COD ID: #9015084) formation in OPC compared to the CSS binder. From Figure 9, it shows that early ettringite formation acted as crack bridge in OPC mortar.

Table 4. Element composition from EDS results.

Elemental Ratios	CSS-Cement Mortar Spectrum 27 Figure 9A	Cement Mortar Spectrum 5 Figure 9B
Ca/Si	5.23	3.08
Ca/C	2.24	2.81
Ca/K	5.34	11.13

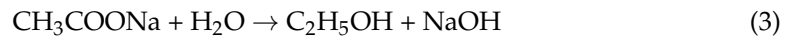
3.5. Effect of Coffee Silverskin on the Bond Vibration in the Blended Mortar

CSS does not cause the disappearance of bound water molecules in the capillary and gel pores of CBM as observed at wavenumbers 3428 , 2926 and 1647 cm^{-1} (Figure 7) when comparing it with the OPC binder, whose peaks were 3418 cm^{-1} , 2922 cm^{-1} and 1655 cm^{-1} , respectively [38]. There is more C-O vibration from CO_2 at 1476 cm^{-1} in the OPC mortar compared to 1427 cm^{-1} in the CBM. The presence of portlandite reaction with atmospheric CO_2 could induce the formation of calcite in both systems, as shown in Equation (2):



In Figure 7, C=O bonds were noticeably present at wavenumber 2344 cm^{-1} in OPC binder due to the presence of calcite (CaCO_3). The bond vibrated at higher frequency at wavenumber 2360 cm^{-1} (Figure 7) in CBM due to the presence of calcite and 5, cafeoylquinc acid in CSS [39]. The bands $960\text{--}1099\text{ cm}^{-1}$ represent the symmetric bending of organic C-H and the bending vibration of Si-O-Si [40]. However, the Si-O-Si bending vibration peak shows a broad weak band that suggests the presence of inorganic compounds in CSS. This means that presence of CSS affected silica organization within the binder,

thereby making CBM more amorphous compared to the OPC binder. This phenomenon necessitated the decrease in the compressive strength. The presence of vibration of $-OH$ at 3642 cm^{-1} indicates the formation of ethanol and portlandite in the CSS-free mortar, while the portlandite could dominate hydroxyl ions in the OPC mortar. The source of hydroxyl compounds apart from the hydration reaction (portlandite) could also be the hydrolysis of sodium acetate to produce ethanol (C_2H_5OH) and sodium hydroxide ($NaOH$), as shown in Equation (3):



3.6. Effect of Coffee Silverskin on Water Absorption of Blended Mortar

From Figure 11, there is a progressive increment in the water absorption capacity of CBM. The maximum absorption of 8.96% was recorded at the CSS/binder ratio of 5%. There is linearity (7.84–8.44%) in the progress of absorption from the CSS/binder increases from 1–3%. The higher absorption recorded in the CSS-blended mortar was due to the presence of microcracks, as shown in Figure 9. The water holding ability and larger surface area of CSS in comparison with OPC could also be contributed to its absorptive capacity. The polygonal shape of the CSS particle could cause proliferation of interfacial transition zone or air pockets with the OPC particle, thereby enhancing microstructural porosity. Despite the larger absorption, there is no physical swelling or disintegration observed in any of the samples. The capacity of CSS-blended mortar to absorb moisture without disintegration could make it suitable for subgrade in road pavement construction. The lower density of CSS-blended mortar in comparison with the OPC mortar implies that it can be used to generate lightweight mortar and concrete.

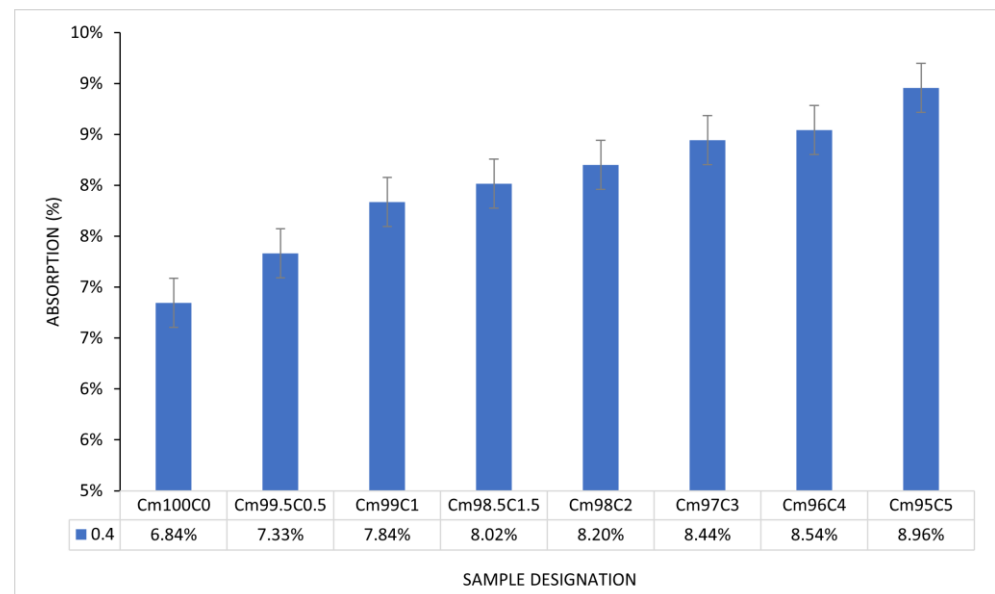


Figure 11. Water absorption of coffee-silverskin-blended mortar.

4. Conclusions

This study has investigated the workability, setting time, absorption and microstructural characteristics of coffee silverskin (CSS)-blended mortar (CBM) prepared by partially replacing ordinary Portland cement (OPC) such that the CSS/(OPC + CSS) ratio ranges from 0 to 5%. The following are the conclusions:

- (1) CSS decreases the workability and setting time in the blended mortar, but early setting does not accelerate the rate of strength development.
- (2) The optimum value of CSS/(OPC + CSS) ratio to produce the maximum 28-day compressive strength mortar was 1%.

- (3) The maximum 3-day (20 MPa) and 28-day (38.5 MPa) strengths of coffee-blended mortar were 25.4% and 7.2%, respectively, less than the maximum strength obtained in the OPC mortar.
- (4) X-ray diffraction identified CSH, anhydrite, CaNaPO₄, calcite and portlandite in CBM.
- (5) CBM has lower Ca/K and Ca/C and higher Ca/Si in comparison with OPC, as observed through the energy dispersive spectroscopy (EDS) results.
- (6) CSS induced microcracks into the matrix of CBM microstructure thereby leading to lower compressive strength in comparison with OPC binder.
- (7) CSS increased water absorption of OPC mortar from 7.93 to 8.96% when cement was partially replaced by 0.5 wt and 5 wt%, respectively.

Author Contributions: Conceptualization, M.O.Y. and Z.M.A.M.; software/characterization, H.D.M. and M.O.Y.; validation, M.O.Y.; formal analysis, M.O.Y. and Z.M.A.M.; investigation, M.O.Y., Z.M.A.M., M.T.S. and A.A.A.; resources, M.O.Y.; data curation, Z.M.A.M.; writing, M.O.Y.; writing and editing, M.O.Y. and A.A.A.; visualization, M.O.Y.; supervision, M.O.Y.; project administration, M.O.Y. and M.O.M.A.; funding acquisition, M.O.Y., Z.M.A.M., M.T.S., M.O.M.A. All authors have read and agreed to the published version of the manuscript.

Funding: The authors extend their appreciation to the Deanship for Research and Innovation, Ministry of Education in Saudi Arabia for funding this research work through the project No: S-0069-1443.

Data Availability Statement: Not applicable.

Acknowledgments: The authors would like to appreciate the remarks of the anonymous reviewers which have greatly improved the manuscript. The continuous support of University of Hafr Al Batin is appreciated.

Conflicts of Interest: The authors declare no conflict of interest.

References

1. Jadhav, R.; Sen, T.K.; Deshpabhu, S. Coffee as a cement retarder. In Proceedings of the SPE Middle East Oil & Gas Show and Conference, Manama, Bahrain, 6–9 March 2017; pp. 308–317. [\[CrossRef\]](#)
2. De Almeida, A.C.; da Silva, M.A.L.; de Abreu, Q.C.; da Silva Martins, A.L.; Ribeiro, S.P.; de Souza Siqueira Pereira, C. Evaluation of Partial Sand Replacement by Coffee Husks in Concrete Production. *J. Environ. Sci. Eng. B* **2019**, *8*, 129–133. [\[CrossRef\]](#)
3. Wondemagegnehu, E.B.; Gupta, N.K.; Habtu, E. Coffee parchment as potential biofuel for cement industries of Ethiopia. *Energy Sources Part A Recover. Util. Environ. Eff.* **2019**, *44*, 5004–5015. [\[CrossRef\]](#)
4. International Coffee Organization (ICO). *Coffee Market Report*; International Coffee Organization: London, UK, 2021.
5. Narita, Y.; Inouye, K. Review on utilization and composition of coffee silverskin. *Food Res. Int.* **2014**, *61*, 16–22. [\[CrossRef\]](#)
6. Cruz, R. Coffee By-Products: Sustainable Agro-Industrial Recovery and Impact on Vegetables Quality. Master's Thesis, Universidade Do Porto, Porto, Portugal, 2014.
7. Anisah, A.; Nugroho, M.; Handoyo, S.S.; Musalamah, S.; Maulana, A.; Ramadhan, M.A.; Sambowo, K.A.; Sumarsono, R.A. Furnace temperature of coffee grounds as organic waste-based cementitious material in concrete. *IOP Conf. Ser. Mater. Sci. Eng.* **2021**, *1098*, 22087. [\[CrossRef\]](#)
8. Blinová, L.; Sirotiak, M.; Bartošová, A.; Soldán, M. Review: Utilization of Waste from Coffee Production. *Res. Pap. Fac. Mater. Sci. Technol. Slovak Univ. Technol.* **2017**, *25*, 91–101. [\[CrossRef\]](#)
9. Górska, A.; Brzezińska, R.; Wirkowska-Wojdyła, M.; Bryś, J.; Domian, E.; Ostrowska-Ligeza, E. Application of thermal methods to analyze the properties of coffee silverskin and oil extracted from the studied roasting by-product. *Appl. Sci.* **2020**, *10*, 8790. [\[CrossRef\]](#)
10. Ballesteros, L.F.; Teixeira, J.A.; Mussatto, S.I. Chemical, Functional, and Structural Properties of Spent Coffee Grounds and Coffee Silverskin. *Food Bioprocess Technol.* **2014**, *7*, 3493–3503. [\[CrossRef\]](#)
11. Hejna, A. Coffee Silverskin as a Potential Bio-Based Antioxidant for Polymer Materials: Brief Review. *Proceedings* **2021**, *69*, 20. [\[CrossRef\]](#)
12. Atabani, A.E.; Al-Muhtaseb, A.H.; Kumar, G.; Saratale, G.D.; Aslam, M.; Khan, H.A.; Said, Z.; Mahmoud, E. Valorization of spent coffee grounds into biofuels and value-added products: Pathway towards integrated bio-refinery. *Fuel* **2019**, *254*, 115640. [\[CrossRef\]](#)
13. Mussatto, S.I.; Carneiro, L.M.; Silva, J.P.A.; Roberto, I.C.; Teixeira, J.A. A study on chemical constituents and sugars extraction from spent coffee grounds. *Carbohydr. Polym.* **2011**, *83*, 368–374. [\[CrossRef\]](#)
14. Wenkui, W.D.; Wengui, L.; Tao, P.Z. A comprehensive review on performance of cementitious and geopolymeric concretes with recycled waste glass as powder, sand or cullet. *Resour. Conserv. Recycl.* **2021**, *172*, 105664.

15. Kumar, A. Extraction of caustic potash from coffee husk: Process optimization through response surface methodology. *Int. J. Chem. Sci.* **2013**, *11*, 1261–1269.
16. De Castro, E.D.; Villela, L.S.; Mendes, L.M.; Mendes, R.F.; Ribeiro, A.G.C.; Guimarães Junior, J.B.; Rabelo, G.F. Analysis of the Coffee Peel Application Over the Soil-Cement Bricks Properties Análise Da Aplicação De Casca De Café Nas Propriedades De Tijolos De Solo-Cimento. *Coffee Sci.* **2019**, *14*, 12–23. [[CrossRef](#)]
17. Reta, Y.; Mahto, S. Experimental Investigation on Coffee Husk Ash as a Partial Replacement of Cement for C-25 concrete. *Cikitungi J. Multidiscip. Res.* **2019**, *6*, 152–158.
18. Ambali, F.; Demissew, A.; Fufa, F.; Assefa, S. Partial Replacement of Cement by Coffee Husk Ash for C-25 Concrete Production. *J. Civ. Eng. Sci. Technol.* **2019**, *10*, 12–21. [[CrossRef](#)]
19. la Scalia, G.; Saeli, M.; Miglietta, P.P.; Micale, R. Coffee biowaste valorization within circular economy: An evaluation method of spent coffee grounds potentials for mortar production. *Int. J. Life Cycle Assess.* **2021**, *26*, 1805–1815. [[CrossRef](#)]
20. Kua, T.A.; Arulrajah, A.; Horpibulsuk, S.; Du, Y.J.; Shen, S.L. Strength assessment of spent coffee grounds-geopolymer cement utilizing slag and fly ash precursors. *Constr. Build. Mater.* **2016**, *115*, 565–575. [[CrossRef](#)]
21. Kristanto, G.A.; Wijaya, H. Assessment of spent coffee ground (SCG) and coffee silverskin (CS) as refuse derived fuel (RDF). *IOP Conf. Ser. Earth Environ. Sci.* **2018**, *195*, 12056. [[CrossRef](#)]
22. *ASTM C150-07*; Standard Specification for Portland Cement. ASTM International: West Conshohocken, PA, USA, 2007.
23. *ASTM C 157*; Standard Test Method for Length Change of Hardened Hydraulic-Cement Mortar and Concrete. ASTM International: West Conshohocken, PA, USA, 2009. [[CrossRef](#)]
24. *ASTM C1437-20*; Standard Test Method for Flow of Hydraulic Cement Mortar. ASTM International: West Conshohocken, PA, USA, 2020.
25. *ASTM C191-21*; Standard Test Methods for Time of Setting of Hydraulic Cement by Vicat Needle. ASTM International: West Conshohocken, PA, USA, 2021.
26. *ASTM C1403-15*; Standard Test Method for Rate of Water Absorption of Masonry Mortars. ASTM International: West Conshohocken, PA, USA, 2015.
27. *ASTM C109/C109M-20*; Standard Test Method for Compressive Strength of Hydraulic Cement Mortars (Using 2-in. or [50-mm] Cube Specimens). ASTM International: West Conshohocken, PA, USA, 2020.
28. Doebelin, N.; Kleeberg, R. Profex: A graphical user interface for the Rietveld refinement program BGMN. *J. Appl. Crystallogr.* **2015**, *48*, 1573–1580. [[CrossRef](#)]
29. *ASTM C192/C192M*; Standard Practice for Making and Curing Concrete Test Specimens in the Laboratory. ASTM International: West Conshohocken, PA, USA, 2016; pp. 1–8.
30. Kemsley, E.K.; Ruault, S.; Wilson, R.H. Discrimination between *Coffea arabica* and *Coffea canephora* variant robusta beans using infrared spectroscopy. *Food Chem.* **1995**, *54*, 321–326. [[CrossRef](#)]
31. Chan, G.K.L.; Witkowski, A.; Gantz, D.L.; Zhang, T.O.; Zanni, M.T.; Jayaraman, S.; Cavigliolo, G. Myeloperoxidase-mediated methionine oxidation promotes an amyloidogenic outcome for apolipoprotein A-I. *J. Biol. Chem.* **2015**, *290*, 10958–10971. [[CrossRef](#)] [[PubMed](#)]
32. Ribeiro, J.S.; Salva, T.J.; Ferreira, M.M.C. Chemometric studies for quality control of processed brazilian coffees using drifts. *J. Food Qual.* **2010**, *33*, 212–227. [[CrossRef](#)]
33. Figueiró, S.D.; Góes, J.C.; Moreira, R.A.; Sombra, A.S.B. On the physico-chemical and dielectric properties of glutaraldehyde crosslinked galactomannan-collagen films. *Carbohydr. Polym.* **2004**, *56*, 313–320. [[CrossRef](#)]
34. Xuan, S.H.; Lee, K.S.; Jeong, H.J.; Park, Y.M.; Ha, J.H.; Park, S.N. Cosmeceutical activities of ethanol extract and its ethyl acetate fraction from coffee silverskin. *Biomater. Res.* **2019**, *23*, 2. [[CrossRef](#)] [[PubMed](#)]
35. Nasti, R.; Galeazzi, A.; Marzorati, S.; Zaccheria, F.; Ravasio, N.; Bozzano, G.L.; Manenti, F.; Verotta, L. Valorisation of Coffee Roasting By-Products: Recovery of Silverskin Fat by Supercritical CO₂ Extraction. *Waste Biomass Valorization* **2021**, *12*, 6021–6033. [[CrossRef](#)]
36. Mota, D.A.; Barbosa, M.D.S.; Schneider, J.K.; Lima, Á.S.; Pereira, M.M.; Krause, L.C.; Soares, C.M.F. Potential Use of Crude Coffee Silverskin Oil in Integrated Bioprocess for Fatty Acids Production. *J. Am. Oil Chem. Soc.* **2021**, *98*, 519–529. [[CrossRef](#)]
37. Bishop, J.L.; Lane, M.D.; Dyar, M.D.; King, S.J.; Brown, A.J.; Swayze, G.A. Spectral properties of Ca-sulfates: Gypsum, bassanite, and anhydrite. *Am. Mineral.* **2014**, *99*, 2105–2115. [[CrossRef](#)]
38. Schneider, U.; Alonso, M.C.; Pimienta, P.; Jansson, R. Physical properties and behaviour of high-performance concrete at high temperatures. In *Structures in Fire: Proceedings of the Sixth International Conference, East Lansing, MI, USA, 2–4 June 2010*; DEstech Publications: Lancaster, PA, USA, 2010; pp. 800–808.
39. Beltran-Medina, E.A.; Guatemala-Morales, G.M.; Corona-González, R.I.; Padilla-Camberos, E.; Mondragó, P.M. Evaluation of the analytical conditions for the determination of chlorogenic acid in coffee silverskin. *Chem. Anal. Chem.* **2019**, 1–7. [[CrossRef](#)]
40. Iriando-DeHond, A.; Ramírez, B.; Escobar, F.V.; del Castillo, M.D. Antioxidant properties of high molecular weight compounds from coffee roasting and brewing byproducts. *Bioact. Compd. Health Dis.* **2019**, *2*, 48–63. [[CrossRef](#)]